Resolving intramolecular-distortion changes induced by the partial fluorination of pentacene adsorbed on Cu(111)

Antoni Franco-Cañellas,[1] Qi Wang,[2,1] Katharina Broch,[1] Bin Shen,[3] Alexander Gerlach,[1] Holger F. Bettinger,[3] Steffen Duhm,[2] and Frank Schreiber[1,*]

[1]*Institut für Angewandte Physik, Universität Tübingen, 72076 Tübingen, Germany*

[2]*Institute of Functional Nano & Soft Materials (FUNSOM) and Jiangsu Key Laboratory for Carbon-Based Functional Materials & Devices, Soochow University, Suzhou 215123, People's Republic of China*

[3]*Institut für Organische Chemie, Universität Tübingen, 72076 Tübingen, Germany*

(Received 11 October 2017; published 4 April 2018)

We experimentally quantify the molecular bending of a partially fluorinated pentacene (PEN) compound, namely 2,3,9,10-tetrafluoropentacene (F4PEN), adsorbed on Cu(111). By means of the x-ray standing wave (XSW) technique, we directly measure the adsorption distance of three inequivalent carbon sites, the fluorine atoms as well as the total and backbone carbon average adsorption distances. The precise positioning of different sites within the carbon core allows us to resolve two adsorption behaviors, namely a PEN-like strong coupling between the backbone and the substrate, and a repulsive interaction involving the fluorinated short molecular edges, which are 0.91 ± 0.09 Å above the central benzene ring. This finding is further supported by additional electronic and in-plane-structure measurements, thus showing that the selective fluorination of a PEN molecule has only a local conformational effect and it is not sufficient to modify its interface properties. Yet, in the multilayer regime, the electronic and growth properties of the film differ completely from those of PEN and its perfluorinated derivative.

DOI: 10.1103/PhysRevMaterials.2.044002

I. INTRODUCTION

Substrate-induced molecular distortions are important to properly account for the interface dipole between a metal electrode and an organic active material [1,2]. They usually involve functional groups with heteroatoms that act as the main channel whereby the electronic and/or chemical coupling with the surface atoms occurs [3–6]. However, the distortion of a hydrocarbon core has not been experimentally probed with the same success [7,8] and, in most cases, it has only been accessible through state-of-the-art density-functional-theory (DFT) calculations [8–10]. In this work, we directly quantify, using the x-ray standing wave (XSW) technique [11–13], the distortion of the hydrocarbon backbone of a partially fluorinated pentacene (PEN) derivative, namely 2,3,9,10-tetrafluoropentacene (F4PEN, $C_{22}F_4H_{10}$) [14–16], vacuum-sublimated on Cu(111). Our measurements (see Ref. [17] for details), performed at the beamline I09 of the Diamond Light Source, yield two clearly different distortion regimes: one involving the central benzene rings that show a gentle curvature of the molecular backbone, the other involving the short-side carbon and fluorine atoms that present a sharp bending, as seen by their radically different adsorption distances. These two distinguishable distortion regimes can be traced back to PEN and its perfluorinated derivative (PFP) deposited on the same surface (Fig. 1). The average carbon adsorption distance of the former is 2.34 Å [18] and presents, as seen in DFT calculations [9], a gentle curvature, whereas the latter has an average carbon height of 2.98 Å [18] and a sharp bending [9]. These two different scenarios raise the question of whether the mild fluorination of the PEN core has an impact on the electronic and in-plane properties as well. To address this, we performed complementary measurements (same setup as in Ref. [19]) of the chemical state by means of x-ray photoelectron spectroscopy (XPS), the electronic properties, using ultraviolet photoelectron spectroscopy (UPS), and the lateral arrangement, as inferred by low-energy electron diffraction (LEED). The set of experimental results shows that the electronic characteristics and the in-plane arrangement of F4PEN (chemical structure in the inset of Fig. 2) in direct contact with the surface remain unaffected by the partial fluorine substitution. Interestingly, measurements for higher coverages hint at completely different electronic and growth properties, compared to PEN and PFP, most likely due to the different molecule-molecule interactions, which are dominated by the directional intramolecular dipole moment.

II. RESULTS AND DISCUSSION

We start by characterizing the chemical state of an F4PEN (sub)monolayer deposited on Cu(111). Figure 2 displays high-resolution XPS (HR-XPS) measurements of the F 1*s* and C 1*s* core levels. The carbon signal shows two distinctive peaks at ∼284.7 eV and ∼286.4 eV. The former, including the large shoulder appearing toward lower binding energies (BEs), is associated with the inequivalent carbon atoms within the molecular backbone, whereas the latter is related to the fluorinated carbon atoms (C-F). This assignment is done following the molecular stoichiometry, in line with previous studies

*frank.schreiber@uni-tuebingen.de

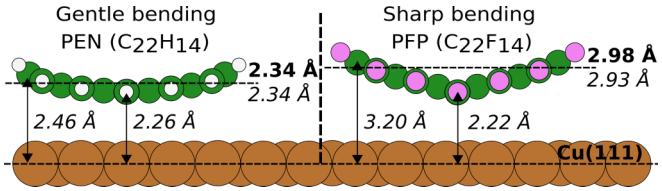

FIG. 1. Sketch of the adsorption geometries of PEN and PFP on Cu(111) as obtained from DFT calculations [9]. The adsorption distances in bold are taken from XSW measurements [18], whereas those in italics correspond to the calculated values [9].

on this molecule [15,16] and PFP [18,20,21]. In addition, at the low-BE edge, there is a small tail that is attributed to a low portion of carbon atoms bound to the substrate (C-Cu), probably belonging to molecules adsorbed close to step edges [20–22]. The fluorine core-level signal, however, does not show any appreciable evidence of defluorination [21], as deduced from the small width and the absence of additional peaks, thus ruling out any significant substrate- or beam-induced [17] effects. The shoulder at the higher BE side of the carbon C-F feature is attributed to shakeup satellites [21,23]. On the other hand, the characteristic line shape of the backbone component, with the pronounced shoulder accompanying the main peak, can be explained by the effect of the substrate on the chemical environment of the different carbon-core atoms, which, depending on the position relative to the copper atoms underneath, undergo different BE shifts. Such an effect has been used to explain the core-level-peak splitting of PEN on different copper (among others [10,24]) surfaces [18,25–27]. In the case of F4PEN, whose hydrogen atoms at the short molecular edges are substituted by fluorine, the C(6) component (C-F) is shifted toward higher BE due to the strong electronegativity of fluorine, thus turning the double peak seen for PEN on Cu(111) [18] into a shoulder. Despite the

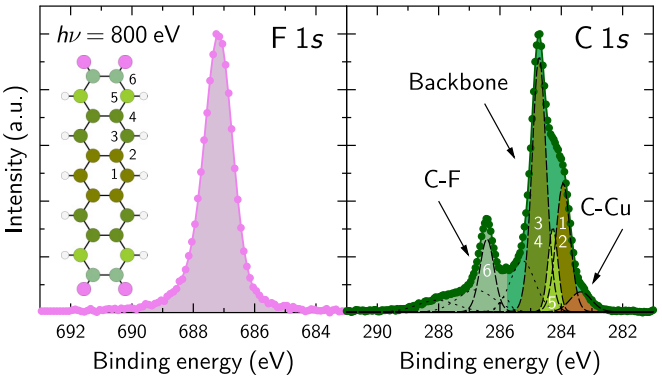

FIG. 2. HR-XPS measurements of the F 1*s* and C 1*s* core levels belonging to an F4PEN (sub)monolayer adsorbed on Cu(111). Inset: molecular structure of F4PEN (fluorine atoms in violet and the resolved inequivalent carbon atoms in different shades of green). Note that the numbering differs from that of the molecular structure (IUPAC nomenclature). For carbon, the areas corresponding to the C-F and the backbone parts are distinguished and the specific components for the different inequivalent carbon species are included (shake-up satellites as dotted lines) [15,16]. Similar areas were used to account for the different photoelectron yields used to evaluate the XSW data in Fig. 4.

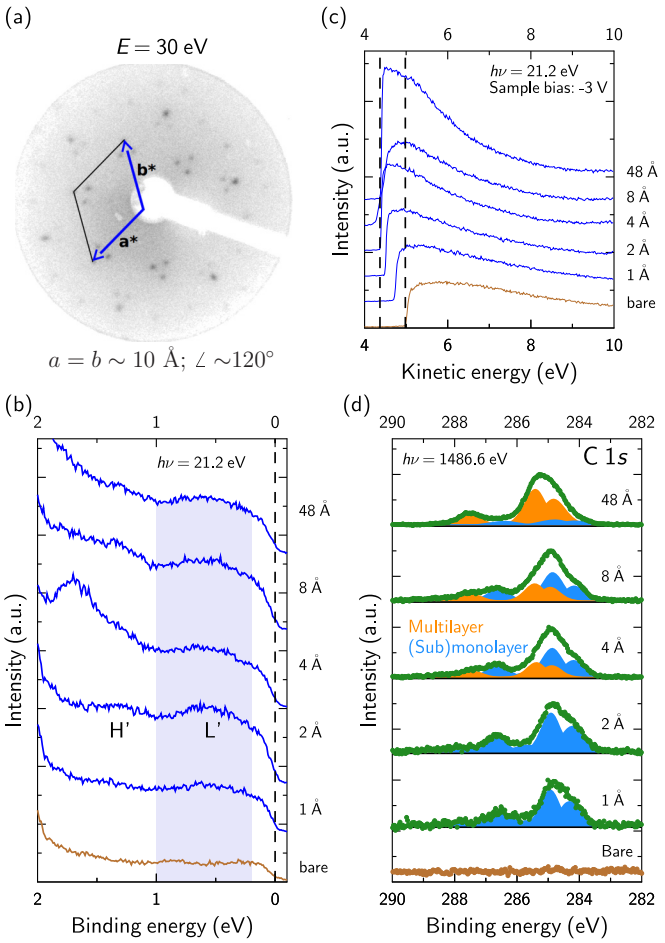

FIG. 3. (a) LEED pattern obtained for an F4PEN nominal coverage of 4 Å. Unit cell superimposed. (b) Coverage-dependent VB spectra: the F-LUMO (L') and the relaxed HOMO (H') are identified for submonolayer coverages. A visible F-LUMO beyond the monolayer is indicative of strong island growth upon wetting-layer(s) formation. (c) Secondary-electron cutoff (SECO) region at different coverages. (d) Coverage-dependent XPS for the carbon signal.

mild fluorination, the backbone curvature that renders slightly inequivalent adsorption sites in the case of PEN [9,10,26] can still be expected, as deduced from the aforementioned shoulder. The precise assignment of the different inequivalent carbon components C(1-5) within the backbone is a difficult task, not exempt from controversy, which ideally would require theoretical input [10,24,28,29]. In our case, the core-level fitting [17] was done in parallel with the XSW analysis, and the structural information obtained from each component was used as a guideline for the peak assignment. This will be explained in more detail below.

The lateral arrangement of F4PEN, within the first monolayer, shows an identical LEED pattern [Fig. 3(a)] such as that reported for PEN on the same substrate [19]. Figure 3(b) shows the coverage-dependent spectra of the valence-band (VB) region close to the Fermi edge as measured by UPS. Up to the monolayer (ML) coverage, the behavior is virtually identical to that of PEN on the same substrate [19]: the former lowest-unoccupied molecular orbital (F-LUMO), centered at ∼0.5 eV, becomes filled by charge transfer (CT)

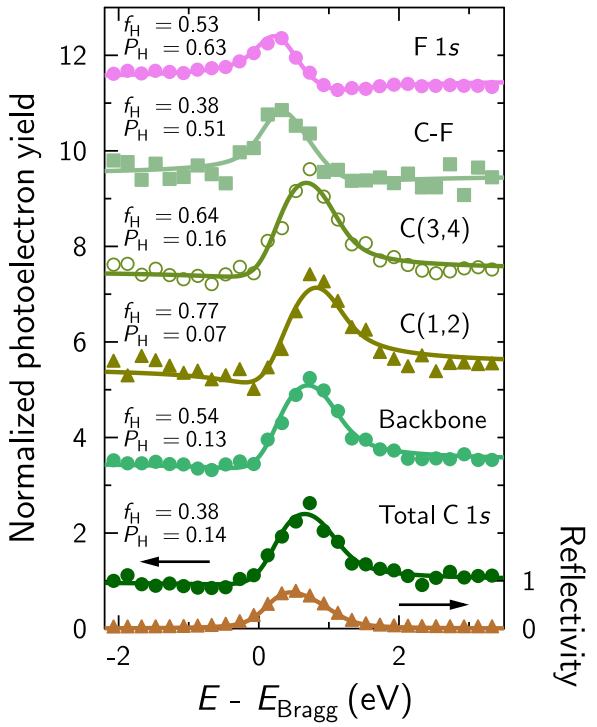

FIG. 4. XSW measurements corresponding to an F4PEN (sub)monolayer adsorbed on Cu(111). The fitting parameters, namely the coherent fraction (f_H) and the coherent position (P_H), are included (see Ref. [17] for details). Note that the different modulation of the photoelectron yield for the F 1s and C-F signals compared to those of the carbon backbone is already an indication of the different adsorption positions.

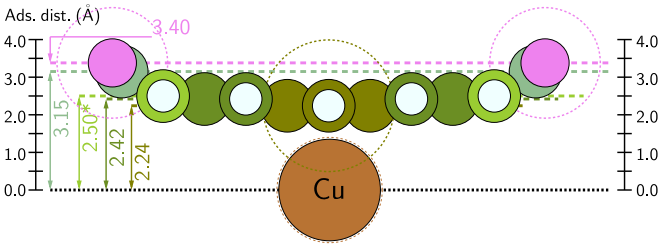

FIG. 5. Sketch of the vertical adsorption geometry of F4PEN on Cu(111) (in Å) as inferred from the XSW measurements (Fig. 4). The dashed circles represent the vdW radii. Note that the adsorption distance of component C(5) (*) is not directly measured but inferred from the vector analysis of the XSW results [17].

from the substrate, and the highest-occupied molecular orbital (HOMO), centered at ∼1.2 eV, relaxes [19]. The vacuum level (VL) decreases by ∼0.60 eV [Fig. 3(c)], which also compares well with PEN (∼0.7 eV [19]). Consequently, from the electronic and in-plane arrangement perspective, F4PEN molecules in direct contact with Cu(111) behave very similar to PEN, indicating a prevalence of the strong backbone-substrate interaction, which is, however, absent in PFP [20]. For higher coverages (nominally 8 and 48 Å) the intensity of secondary electrons increases [Fig. 3(c)], but the valence electron spectra hardly change [Figs. 3(b) and S1] pointing to pronounced Stranski-Krastanov growth (island formation on a wetting layer). This is in line with XPS measurements at the same coverages, where the layer in contact with the substrate can still be distinguished from the multilayer contribution [Fig. 3(d)] [30]. Compared to PEN, where a pronounced HOMO peak from crystalline PEN in multilayers has been measured for similar coverages [19], both the growth and the electronic properties of the multilayer regime are in remarkable contrast to those shown here for F4PEN. It is plausible to think that, released from the dominant substrate bonding, the molecules in the subsequent layers are given the freedom to rearrange in a more favorable configuration, most likely dominated by the presence of the electronegative fluorine atoms and their induced intramolecular dipole [31,32].

Having established a detailed picture for the chemical, electronic, and in-plane characteristics of F4PEN on Cu(111), we discuss the vertical adsorption geometry obtained by the XSW technique [13]. The measurements, performed in backreflection geometry, record the x-ray reflectivity of the sample and the photoelectron yield Y_P (obtained from the peak/component area evaluation in an XPS scan), at different photon energies around the (111) Bragg peak ($E_{Bragg} \sim 2.97$ keV). From the data fitting, two output parameters contain the structural information of the adsorbate: the coherent position (P_H), which is directly related to the adsorption distance for a given chemical species via $d_H = d_0(n + P_H)$ [11], where d_0 is the lattice plane spacing of copper along the H = [111] direction and n is an integer number [11], and the coherent fraction (f_H), which contains information about the vertical ordering of a given species around its mean adsorption distance ($f_H = 0$ for randomly distributed emitters and $f_H = 1$ for the case in which the atoms are all at the same adsorption distance). Y_P is obtained for each chemical element and can be resolved for inequivalent species within a given signal provided that the core-level model employed renders coherent modulations for the individual fitting components. Consequently, this can be regarded as an independent test for the core-level fitting that is used to extract Y_P. Furthermore, f_H can also be considered as a parameter to discriminate between models since adsorption distances associated with high coherent fractions are generally more meaningful.

In this context, several fitting models (with a varying number of components to account for the backbone signal) based on the molecular stoichiometry and previous studies of PEN [18,20,26,30] and some of its derivatives [23] were used to extract Y_P. The model shown in Fig. 2 represents the case that best reproduced the C 1s core-level signal and also rendered coherently-modulated Y_P curves (Fig. 4) with the highest f_H for the main fitting components. Thus, thanks to both the high-quality data and the core-level fitting model employed, we are able to directly evaluate the adsorption distance of three inequivalent carbon sites, namely components C(1,2), C(3,4), and C-F [C(6)], and indirectly we infer a fourth one, component C(5) [17]. Together with the position of the fluorine atoms and the total and backbone carbon average adsorption distances, we obtain a very precise dissection of the different adsorption distances contributing to the overall molecular bending (sketch in Fig. 5): the position of the C-F carbon atoms, 3.15 ± 0.05 Å, compared to those at the center [component C(1,2)], 2.24 ± 0.08 Å, renders a carbon bottom-to-top vertical distance of

0.91 ± 0.09 Å, which accounts for a remarkable molecular distortion (in line with the even higher fluorine position, 3.40 ± 0.02 Å). Yet, the fact that the average carbon distance (Total C 1*s* in Fig. 4), 2.37 ± 0.04 Å, is virtually the same as the average backbone one, 2.36 ± 0.02 Å, is quite unexpected for a carbon spread of ∼0.9 Å. This can be explained by considering the adsorption distance of the other inequivalent carbon atoms, namely C(3,4) (2.42 ± 0.02 Å) and C(5) (2.50 ± 0.36 Å), both being close to the mean carbon distance, and thus pointing toward a rather gentle bending of the central benzene rings composing the F4PEN backbone. Consequently, the XSW analysis shows that the remarkable sharp bending of F4PEN is almost entirely localized at the fluorinated edges, since the backbone only shows a slight curvature. This appears in stark contrast to early DFT calculations with semiempirical van der Waals (vdW) corrections performed on the same system, where an overall carbon bending of ∼0.3 Å was reported [33]. Interestingly, our measured C-F adsorption distance is very similar to that of the short edge of PFP calculated using a more recent vdW-corrected density functional [9], whereas the central benzene ring and the average carbon distances match those reported for PEN [9,18] (Fig. 1), further supporting the two differentiated adsorption behaviors.

We note that the particular labeling of the C(1-5) components used to fit the C 1*s* signal was redefined *a posteriori*, based on the adsorption distances obtained from each one and considering their relatively high coherent fractions that indicate a homogeneous distribution of the atoms contributing to them. Hence, the main components were assigned to different benzene rings rather than to C-C and C-H carbon atoms as done elsewhere for PEN [26]. In either case, it is important to clarify that the adsorption distances and the derived adsorption geometry described above are independent from the particular labeling of the core-level components and only depend on how Y_P is evaluated, i.e., the particular fitting model.

Any type of adsorption-induced distortion comes out of the balance between Pauli repulsion and attractive forces, namely chemical bonding stemming from molecule-substrate orbital hybridization (and/or CT) and vdW forces. In acenes, the most reactive part is the central benzene ring that is, therefore, more prone to hybridization than the short-edge carbons, which are comparatively less affected by the surface, thus explaining its small upward curvature reported for PEN [7–9]. Fluorination increases the repulsion, via F $2p$ orbitals, with the substrate [33], as is well exemplified in the comparison of PEN and PFP (Fig. 1). Hence, considering the adsorption geometry reported here for F4PEN, it is clear that the increased repulsion exerted by the selective fluorine substitution is not sufficient to lift the PEN-like backbone geometry, and its effect is localized at the short edges.

III. SUMMARY AND CONCLUSIONS

In summary, our precise measurements of the adsorption distance of different inequivalent carbon species allow the distortion of F4PEN in contact with Cu(111) to be experimentally quantified. The selective fluorination of the short molecular edges renders two markedly different adsorption behaviors within the molecule. The first one comprises the carbon backbone, which is dominated by a strong coupling with the substrate, as denoted by the presence of CT features in the VB and the very short adsorption distance of the central benzene rings. The second one involves the fluorinated edges, which show a repulsive interaction with the copper atoms, as deduced from their much higher adsorption distance compared to the central ring, yielding an overall carbon bottom-to-top distance of ∼0.9 Å. Despite this remarkable carbon spread, the measured inequivalent carbon positions, as well as the average carbon adsorption distances, indicate that the central benzene rings are just gently curved, similarly to PEN. Therefore, it is mostly the short-edge carbon atoms attached to fluorine that account for the sharp bending. Considering all structural and electronic data, it can be concluded that the increased repulsion rendered by the four fluorine atoms is not sufficient to lift the strong electronic coupling of the PEN backbone with the copper substrate, and its effect is only localized at the molecular short edges. Interestingly, our results for higher coverages show a different growth behavior and electronic properties for F4PEN compared to PEN [18,19] (and PFP [18,20]) adsorbed on Cu(111).

The results reported here represent a step forward to a full experimental atomistic description of the adsorption geometry of a π-conjugated molecule adsorbed on a metal substrate and, in particular, the conformational changes induced by the interplay between attractive and repulsive forces acting on the adsorbate. For the case studied here, a partially fluorinated PEN molecule, we provide insights on the effect of fluorination at the molecule-metal interface, as well as in the multilayer regime. Last but not least, the fact that a particular core-level model can be related to the quality of the XSW analysis may be regarded as an independent way to verify it.

ACKNOWLEDGMENTS

The authors thank the Diamond Light Source for access to beamline I09, and its staff for excellent support during the beamtime. Special thanks to D. A. Duncan, who also commented on the manuscript. Financial support from the Soochow University–Western University Center for Synchrotron Radiation Research, the Collaborative Innovation Center of Suzhou Nano Science & Technology (NANO-CIC), and the Deutsche Forschungsgemeinschaft (DFG) is gratefully acknowledged. B.S. gratefully acknowledges support from the China Scholarship Council.

[1] R. Otero, A. L. Vázquez de Parga, and J. M. Gallego, Surf. Sci. Rep. **72**, 105 (2017).

[2] R. J. Maurer, V. G. Ruiz, J. Camarillo-Cisneros, W. Liu, N. Ferri, K. Reuter, and A. Tkatchenko, Prog. Surf. Sci. **91**, 72 (2016).

[3] A. Hauschild, K. Karki, B. C. C. Cowie, M. Rohlfing, F. S. Tautz, and M. Sokolowski, Phys. Rev. Lett. **94**, 036106 (2005).

[4] G. Heimel, S. Duhm, I. Salzmann, A. Gerlach, A. Strozecka, J. Niederhausen, C. Bürker, T. Hosokai, I. Fernandez-Torrente, G. Schulze, S. Winkler, A. Wilke, R. Schlesinger, J. Frisch, B. Bröker, A. Vollmer, B. Detlefs, J. Pflaum, S. Kera, K. J. Franke, N. Ueno, J. I. Pascual, F. Schreiber, and N. Koch, Nat. Chem. **5**, 187 (2013).

[5] M. Willenbockel, D. Lüftner, B. Stadtmüller, G. Koller, C. Kumpf, S. Soubatch, P. Puschnig, M. G. Ramsey, and F. S. Tautz, Phys. Chem. Chem. Phys. **17**, 1530 (2014).

[6] A. Franco-Cañellas, Q. Wang, K. Broch, D. A. Duncan, P. K. Thakur, L. Liu, S. Kera, A. Gerlach, S. Duhm, and F. Schreiber, Phys. Rev. Mater. **1**, 013001(R) (2017).

[7] L. Gross, F. Mohn, N. Moll, P. Liljeroth, and G. Meyer, Science **325**, 1110 (2009).

[8] B. Schuler, W. Liu, A. Tkatchenko, N. Moll, G. Meyer, A. Mistry, D. Fox, and L. Gross, Phys. Rev. Lett. **111**, 106103 (2013).

[9] X.-Q. Shi, Y. Li, M. A. Van Hove, and R.-Q. Zhang, J. Phys. Chem. C **116**, 23603 (2012).

[10] A. Baby, H. Lin, G. P. Brivio, L. Floreano, and G. Fratesi, Beilstein J. Nanotechnol. **6**, 2242 (2015).

[11] J. Zegenhagen, Surf. Sci. Rep. **18**, 202 (1993).

[12] L. Cheng, P. Fenter, M. J. Bedzyk, and N. C. Sturchio, Phys. Rev. Lett. **90**, 255503 (2003).

[13] A. Gerlach, C. Bürker, T. Hosokai, and F. Schreiber, in *The Molecule-Metal Interface*, edited by N. Koch, N. Ueno, and A. T. S. Wee (Wiley-VCH, Weinheim, 2013), pp. 153–172.

[14] B. Shen, T. Geiger, R. Einholz, F. Reicherter, S. Schundelmeier, C. Maichle-Mössmer, B. Speiser, and H. F. Bettinger, J. Org. Chem. **83**, 3149 (2018).

[15] S.-A. Savu, G. Biddau, L. Pardini, R. Bula, H. F. Bettinger, C. Draxl, T. Chassé, and M. B. Casu, J. Phys. Chem. C **119**, 12538 (2015).

[16] S.-A. Savu, A. Sonström, R. Bula, H. F. Bettinger, T. Chassé, and M. B. Casu, ACS Appl. Mater. Interfaces **7**, 19774 (2015).

[17] See Supplemental Material at http://link.aps.org/supplemental/10.1103/PhysRevMaterials.2.044002 for a comprehensive explanation of the experimental details, the XSW technique as well as a discussion of possible beam-damage effects. Also, additional UPS measurements and the vector analysis of the XSW data are included.

[18] N. Koch, A. Gerlach, S. Duhm, H. Glowatzki, G. Heimel, A. Vollmer, Y. Sakamoto, T. Suzuki, J. Zegenhagen, J. P. Rabe, and F. Schreiber, J. Am. Chem. Soc. **130**, 7300 (2008).

[19] M.-C. Lu, R.-B. Wang, A. Yang, and S. Duhm, J. Phys.: Condens. Matter **28**, 094005 (2016).

[20] H. Glowatzki, G. Heimel, A. Vollmer, S. L. Wong, H. Huang, W. Chen, A. T. S. Wee, J. P. Rabe, and N. Koch, J. Phys. Chem. C **116**, 7726 (2012).

[21] C. Schmidt, T. Breuer, S. Wippermann, W. G. Schmidt, and G. Witte, J. Phys. Chem. C **116**, 24098 (2012).

[22] A. Basagni, L. Ferrighi, M. Cattelan, L. Nicolas, K. Handrup, L. Vaghi, A. Papagni, F. Sedona, C. D. Valentin, S. Agnoli, and M. Sambi, Chem. Commun. **51**, 12593 (2015).

[23] S.-A. Savu, M. B. Casu, S. Schundelmeier, S. Abb, C. Tönshoff, H. F. Bettinger, and T. Chassé, RSC Adv. **2**, 5112 (2012).

[24] A. Ugolotti, S. S. Harivyasi, A. Baby, M. Dominguez, A. L. Pinardi, M. F. López, J. Á. Martín-Gago, G. Fratesi, L. Floreano, and G. P. Brivio, J. Phys. Chem. C **121**, 22797 (2017).

[25] O. McDonald, A. Cafolla, Z. Li, and G. Hughes, Surf. Sci. **600**, 1909 (2006).

[26] C. Baldacchini, F. Allegretti, R. Gunnella, and M. G. Betti, Surf. Sci. **601**, 2603 (2007).

[27] M. Chiodi, L. Gavioli, M. Beccari, V. Di Castro, A. Cossaro, L. Floreano, A. Morgante, A. Kanjilal, C. Mariani, and M. G. Betti, Phys. Rev. B **77**, 115321 (2008).

[28] M. Alagia, C. Baldacchini, M. G. Betti, F. Bussolotti, V. Carravetta, U. Ekström, C. Mariani, and S. Stranges, J. Chem. Phys. **122**, 124305 (2005).

[29] K. Diller, R. J. Maurer, M. Müller, and K. Reuter, J. Chem. Phys. **146**, 214701 (2017).

[30] D. G. de Oteyza, Y. Wakayama, X. Liu, W. Yang, P. L. Cook, F. J. Himpsel, and J. E. Ortega, Chem. Phys. Lett. **490**, 54 (2010).

[31] I. Salzmann, A. Moser, M. Oehzelt, T. Breuer, X. Feng, Z.-Y. Juang, D. Nabok, R. G. Della Valle, S. Duhm, G. Heimel, A. Brillante, E. Venuti, I. Bilotti, C. Christodoulou, J. Frisch, P. Puschnig, C. Draxl, G. Witte, K. Müllen, and N. Koch, ACS Nano **6**, 10874 (2012).

[32] G. D'Avino, L. Muccioli, F. Castet, C. Poelking, D. Andrienko, Z. G. Soos, J. Cornil, and D. Beljonne, J. Phys.: Condens. Matter **28**, 433002 (2016).

[33] K. Toyoda, I. Hamada, S. Yanagisawa, and Y. Morikawa, Org. Elec. **12**, 295 (2011).